Article

Phosphorylation Effects on cis/trans Isomerization and the Backbone Conformation of Serine–Proline Motifs: Accelerated Molecular Dynamics Analysis

Donald Hamelberg, Tongye Shen, and J. Andrew McCammon

J. Am. Chem. Soc., **2005**, 127 (6), 1969-1974• DOI: 10.1021/ja0446707 • Publication Date (Web): 20 January 2005

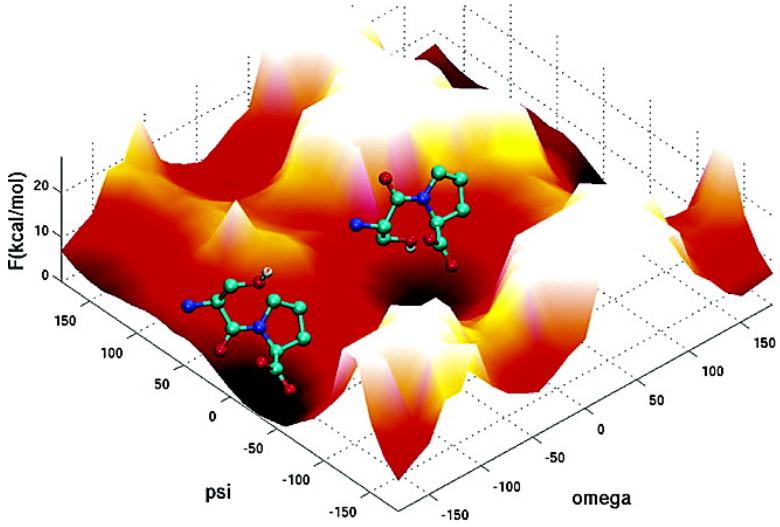

More About This Article

Additional resources and features associated with this article are available within the HTML version:

- Supporting Information
- Links to the 14 articles that cite this article, as of the time of this article download
- Access to high resolution figures
- Links to articles and content related to this article
- Copyright permission to reproduce figures and/or text from this article

View the Full Text HTML

J|A|C|S
ARTICLES
Published on Web 01/20/2005

Phosphorylation Effects on cis/trans Isomerization and the Backbone Conformation of Serine−Proline Motifs: Accelerated Molecular Dynamics Analysis

Donald Hamelberg,*,† Tongye Shen, and J. Andrew McCammon†,‡

Contribution from the Howard Hughes Medical Institute, Center for Theoretical Biological Physics, Department of Chemistry and Biochemistry, and Department of Pharmacology, University of California at San Diego, La Jolla, California 92093-0365

Received September 2, 2004; E-mail: dhamelbe@mccammon.ucsd.edu

Abstract: The presence of serine/threonine−proline motifs in proteins provides a conformational switching mechanism of the backbone through the cis/trans isomerization of the peptidyl−prolyl (ω) bond. The reversible phosphorylation of the serine/threonine modulates this switching in regulatory proteins to alter signaling and transcription. However, the mechanism is not well understood. This is partly because cis/trans isomerization is a very slow process and, hence, difficult to study. We have used our accelerated molecular dynamics method to study the cis/trans proline isomerization, preferred backbone conformation of a serine−proline motif, and the effects of phosphorylation of the serine residue. We demonstrate that, unlike normal molecular dynamics, the accelerated molecular dynamics allows for the system to escape very easily from the trans isomer to cis isomer, and vice versa. Moreover, for both the unphosphorylated and phosphorylated peptides, the statistical thermodynamic properties are recaptured, and the results are consistent with experimental values. Isomerization of the proline ω bond is shown to be asymmetric and strongly dependent on the ψ backbone angle before and after phosphorylation. The rates of escape decrease after phosphorylation. Also, the α-helical backbone conformation is more favored after phosphorylation. This accelerated molecular dynamics approach provides a general approach for enhancing the conformational transitions of molecular systems without having prior knowledge of the location of the minima and barriers on the potential-energy landscape.

Introduction

Complex systems are often characterized by rough and complicated energy landscapes.[1] Such features can yield complicated dynamics evolving over long time scales. The occurrences of large displacements and transitions over high free-energy barriers typically have small probabilities. Though rare, such events are often important compared with higher frequency fluctuations. There are many examples of such cases in chemical and biological systems, including the switching of states of bistable systems or systems with multiple (meta)stable states, such as one sees in protein conformational changes[2] in the regulation of cellular components. However, while it is relatively easy to study dynamics on short time scales (typically at nanoseconds to microseconds for biomolecules) using simulations,[3] it is painful to extend the naïve molecular dynamics simulations to the long time scales that are often of biological interest (often as long as microseconds to seconds for biomolecular systems).

Therefore, an urgent question in computational chemistry and biology is how can barrier crossing events be facilitated using a simulation method, like molecular dynamics (MD), while maintaining (or possibly later capturing) the statistical thermodynamic properties of the system? Several methods have been developed to address this problem, including conformational flooding,[4] replica exchange,[5] self-guided MD,[6] targeted MD,[7] umbrella sampling,[8] locally enhanced sampling,[9] high-temperature MD,[10] multicanonical method,[11] leap dynamics,[12] and others reviewed by Berne and Straub.[13] However, some of these approaches require prior knowledge of the potential-energy landscape of the system. Also, some involve increasing the temperature of the system, thus overestimating the entropic part of the free energy by facilitating transitions that might not be observed at low temperature. In addition, some other methods involve joint approaches that combine several other techniques.

† Department of Chemistry and Biochemistry.
‡ Department of Pharmacology.

(1) Wales, D. J. *Energy Landscapes*; Cambridge University Press: Cambridge, 2003.
(2) Frauenfelder, H.; Sligar, S. G.; Wolynes, P. G. *Science* **1991**, *254*, 1598−1603.
(3) Karplus, M.; McCammon, J. A. *Nat. Struct. Biol.* **2002**, *9*, 646−652.
(4) Grubmuller, H. *Phys. Rev. E* **1995**, *52*, 2893−2906.
(5) Sugita, Y.; Okamoto, Y. *Chem. Phys. Lett.* **2000**, *329*, 261−270.
(6) Wu, X. W.; Wang, S. M. *J. Chem. Phys.* **1999**, *110*, 9401−9410.
(7) Schlitter, J.; Engels, M.; Kruger, P.; Jacoby, E.; Wollmer, A. *Mol. Simul.* **1993**, *10*, 291−308.
(8) Torrie, G. M.; Valleau, J. P. *J. Comput. Phys.* **1977**, *23*, 187−199.
(9) Elber, R.; Karplus, M. *J. Am. Chem. Soc.* **1990**, *112*, 9161−9175.
(10) Bruccoleri, R. E.; Karplus, M. *Biopolymers* **1990**, *29*, 1847−1862.
(11) Bhattacharya, K. K.; Sethna, J. P. *Phys. Rev. A* **1998**, *57*, 2553−2562.
(12) Kleinjung, J.; Bayley, P.; Fraternali, F. *FEBS Lett.* **2000**, *470*, 257−262.
(13) Berne, B. J.; Straub, J. E. *Curr. Opin. Struct. Biol.* **1997**, *7*, 181−189.

10.1021/ja0446707 CCC: $30.25

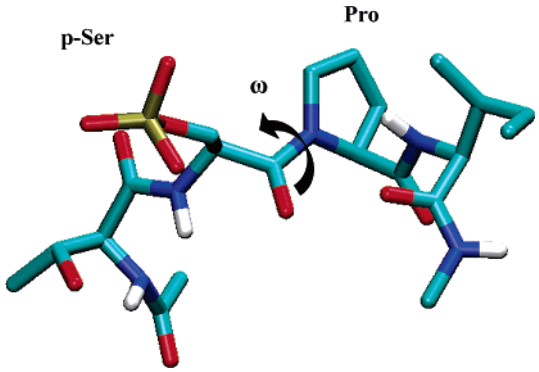

Figure 1. Ace-TpSPI-Nme motif with the peptidyl−prolyl (ω) angle depicted in the trans conformation.

Alternatively, we have introduced an all-atom molecular dynamics technique that avoids some of these shortcomings and can accelerate simulations such that rare events can be observed repetitively, and at the same time, recovers the Boltzmann canonical distribution[14] of the systems. The underlying principle of our method is based on earlier work by Voter[15,16] and other subsequent studies.[17−21] It can accelerate the simulations *without* tuning the force-field parameters or requiring prior knowledge of the locations of the potential-energy basins and transition paths.

To show the strength and robustness of this simulation technique, we have used it to study proline cis/trans isomerization of the peptidyl−prolyl (ω) bond[22] of the serine−proline motif (Figure 1) and the effect of phosphorylation[23] on this isomerization[24,25] and the backbone conformation. The local backbone switching of proline motifs due to the cis/trans isomerization of the ω bond can be the rate-limiting step in protein folding.[26,27] Furthermore, phosphorylation of the serine or threonine regulates important processes in many proteins. The discovery of the enzyme peptidyl−prolyl cis/trans isomerase (Pin1), which specifically binds and catalyzes the isomerization of phosphorylated serine/threonine−proline motifs,[28] has further increased the biological significance of these motifs. The peptidyl−prolyl cis/trans isomerase enzyme has been shown to regulate the conformation and function of some phosphorylated proteins involved in cell mitosis[29] and Alzheimer's disease.[30] The time scale of a single isomerization event is notoriously long (around $10-10^3$ s, corresponding to a barrier height of 15−20 kcal/mol), as was previously measured.[24,25,31] This makes proline isomerization difficult to study even experimentally, especially when the conformational statistics of a single molecule are under consideration. Therefore, many researchers have tended to pick proteins that do not have the complications of cis/trans proline isomerization when studying protein dynamics. However, this slow process is biologically important[25] as it is involved in regulatory pathways. While such processes are difficult to study experimentally, they are almost impossible to observe in realistic time frames with the traditional all-atom simulation techniques. We demonstrate that our accelerated MD method can simulate the barrier crossing transition with ease, and that this method is not limited by system size or solvation model. Therefore, it opens the door to the simulations of the long-time dynamics of complex systems with atomistic details.

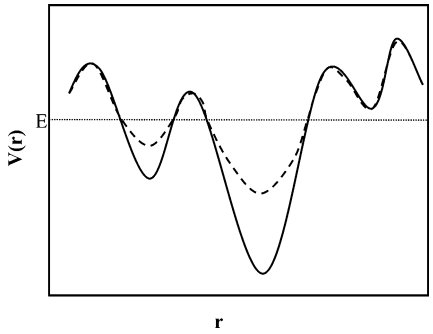

Figure 2. Schematic representation of the normal potential, the modified potential, and the threshold boost energy, *E*.

Theoretical Considerations and Methods

We begin, by reviewing the basis of accelerated MD, to set the stage for several elaborations. If we consider a potential function $V(\mathbf{r})$, represented (solid line) in Figure 2, the average time $t(\mathbf{r})$ spent in a small subdomain at $\mathbf{r}$ is proportional to the Boltzmann probability of being at $\mathbf{r}$, that is, $e^{-\beta V(\mathbf{r})}$. Therefore, if a modified potential $V^*(\mathbf{r})$ is defined (dashed line, Figure 2) such that $V(\mathbf{r}) \leq V^*(\mathbf{r})$, the average time $t^*(\mathbf{r})$ spent in the small subdomain of $V^*(\mathbf{r})$ should also be proportional to the Boltzmann factor, $e^{-\beta V^*(\mathbf{r})}$. Hence, the average time spent in wells of $V^*(\mathbf{r})$ will be less than that spent in corresponding wells of $V(\mathbf{r})$, thus allowing the system to escape to other potential-energy wells in fewer computational steps by modifying the potential surface from $V(\mathbf{r})$ to $V^*(\mathbf{r})$. This can be achieved by adding a continuous non-negative bias potential $\Delta V(\mathbf{r})$ to $V(\mathbf{r})$ in order to get $V^*(\mathbf{r})$, as depicted in Figure 2.

One of the main objectives of this technique that sets it apart from other methods is the construction of the bias potential without prior knowledge of the potential-energy minima and saddle points. In Voter's implementation of the bias potential,[15,16] the Hessian matrix is diagonalized on the fly of the simulation at each step, so that the transition state regions can be identified. However, this approach limits its use to small systems because of its computational cost. To extend the application to much larger systems, a simpler implementation is devised.[14,18−20] A boost energy, E, is chosen such that the simulation is performed on the modified potential $V^*(\mathbf{r}) = V(\mathbf{r}) + \Delta V(\mathbf{r})$ (represented by dashed lines in Figure 2) when $V(\mathbf{r})$ is below E and is performed on the true potential $V^*(\mathbf{r}) = V(\mathbf{r})$ when $V(\mathbf{r})$ is greater than E. This will lead to an enhanced escape rate.

After the simulation on the modified potential-energy landscape, the correct canonical averages of any observable can be recovered by

(14) Hamelberg, D.; Mongan, J.; McCammon, J. A. *J. Chem. Phys.* **2004**, *120*, 11919−11929.
(15) Voter, A. F. *Phys. Rev. Lett.* **1997**, *78*, 3908−3911.
(16) Voter, A. F. *J. Chem. Phys.* **1997**, *106*, 4665−4677.
(17) Gong, X. G.; Wilkins, J. W. *Phys. Rev. B* **1999**, *59*, 54−57.
(18) Pal, S.; Fichthorn, K. A. *Chem. Eng. J.* **1999**, *74*, 77−83.
(19) Rahman, J. A.; Tully, J. C. *J. Chem. Phys.* **2002**, *116*, 8750−8760.
(20) Steiner, M. M.; Genilloud, P. A.; Wilkins, J. W. *Phys. Rev. B* **1998**, *57*, 10236−10239.
(21) Wang, J. C.; Pal, S.; Fichthorn, K. A. *Phys. Rev. B* **2001**, 6308.
(22) Stewart, D. E.; Sarkar, A.; Wampler, J. E. *J. Mol. Biol.* **1990**, *214*, 253−260.
(23) Shen, T. Y.; Wong, C. F.; McCammon, J. A. *J. Am. Chem. Soc.* **2001**, *123*, 9107−9111.
(24) Reimer, U.; Scherer, G.; Drewello, M.; Kruber, S.; Schutkowski, M.; Fischer, G. *J. Mol. Biol.* **1998**, *279*, 449−460.
(25) Schutkowski, M.; Bernhardt, A.; Zhou, X. Z.; Shen, M. H.; Reimer, U.; Rahfeld, J. U.; Lu, K. P.; Fischer, G. *Biochemistry* **1998**, *37*, 5566−5575.
(26) Schmid, F. X.; Baldwin, R. L. *J. Mol. Biol.* **1979**, *133*, 285−287.
(27) Schmid, F. X.; Baldwin, R. L. *Proc. Natl. Acad. Sci. U.S.A.* **1978**, *75*, 4764−4768.
(28) Yaffe, M. B.; Schutkowski, M.; Shen, M. H.; Zhou, X. Z.; Stukenberg, P. T.; Rahfeld, J. U.; Xu, J.; Kuang, J.; Kirschner, M. W.; Fischer, G.; Cantley, L. C.; Lu, K. P. *Science* **1997**, *278*, 1957−1960.
(29) Lu, K. P.; Hanes, S. D.; Hunter, T. *Nature* **1996**, *380*, 544−547.
(30) Lu, P. J.; Wulf, G.; Zhou, X. Z.; Davies, P.; Lu, K. P. *Nature* **1999**, *399*, 784−788.
(31) Fischer, S.; Dunbrack, R. L.; Karplus, M. *J. Am. Chem. Soc.* **1994**, *116*, 11931−11937.

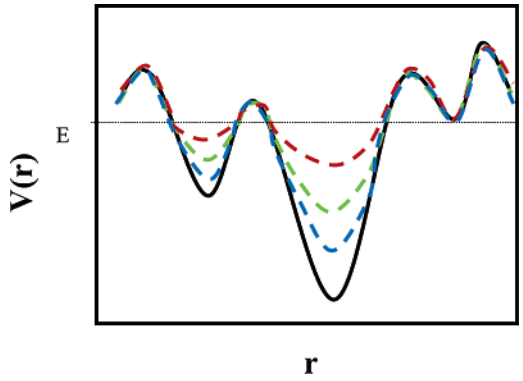

Figure 3. Schematic representation of the normal potential and several bias potentials at fixed threshold boost energy (E) with varying values of α. The α value of the red dashed line is less than that of the green, which is less than that of the blue.

reweighting. The equilibrium ensemble average value of an observable $A(\mathbf{r})$ on the normal potential $V(\mathbf{r})$ is given by eq 1:

$$\langle A \rangle = \frac{\int d\mathbf{r} A(\mathbf{r}) e^{-\beta V(\mathbf{r})}}{\int d\mathbf{r} e^{-\beta V(\mathbf{r})}} \tag{1}$$

Similarly, the ensemble average value of this observable $A(\mathbf{r})$ taken on the modified potential $V^*(\mathbf{r})$ can be written as (substituting for $V^*(\mathbf{r})$)

$$\langle A^* \rangle = \frac{\int d\mathbf{r} A(\mathbf{r}) e^{-\beta V(\mathbf{r}) - \beta \Delta V(\mathbf{r})}}{\int d\mathbf{r} e^{-\beta V(\mathbf{r}) - \beta \Delta V(\mathbf{r})}} \tag{2}$$

Therefore, by reweighting the phase space of the modified potential by multiplying each configuration by the strength of the bias, $e^{\beta \Delta V(\mathbf{r})}$, at each point, the corrected ensemble average, which is equivalent to the average equilibrium observable of $A(\mathbf{r})$ on the normal potential, is obtained.

This scheme is defined in eqs 3 and 4. They relate the modified potential $V^*(\mathbf{r})$ to the true potential $V(\mathbf{r})$, bias potential $\Delta V(\mathbf{r})$, and boost energy E.

$$V^*(\mathbf{r}) = V(\mathbf{r}) + \Delta V(\mathbf{r}) \tag{3}$$

$$\Delta V(\mathbf{r}) = \begin{cases} 0, & V(\mathbf{r}) \geq E \\ f(\mathbf{r}), & V(\mathbf{r}) < E \end{cases} \tag{4}$$

where in our implementation,[14] $f(\mathbf{r})$ is defined as

$$f(\mathbf{r}) = \frac{(E - V(\mathbf{r}))^2}{\alpha + (E - V(\mathbf{r}))} \tag{5}$$

This definition ensures behavior, as shown by the dashed line in Figure 2, such that the derivative of $V^*(\mathbf{r})$ with respect to $\mathbf{r}$ will not be discontinuous at points where $V(\mathbf{r}) = E$. Selection of E and α is important to the method and determines the extent to which the molecular dynamics will be accelerated. While varying the value of α at a constant value of E, the modified potential becomes smoother as α is decreased. Conversely, the modified potential surface becomes rougher as α is increased and matches that of the original surface at a very large value of α, as depicted in Figure 3.

The biased potential, therefore, smooths the local roughness and lowers the barriers of the potential-energy landscape, thus increasing the escape rate of the system from potential-energy basins. The state-to-state evolution of the system on the modified potential occurs at an accelerated rate. Therefore, the higher the boost energy E and the smaller the value of α, the greater the acceleration. The α should, therefore, be given as a positive nonzero value, as previously described,[14] so that the modified potential is not flat, discontinuous where $V(\mathbf{r}) = E$, and echoes the shape of the underlying potential.

A tetrapeptide, Ace-TSPI−Nme, was used to carry out these simulations. This short piece was taken from the NFAT1 protein that has several repeats of the XSPX motif around the calcineurin-binding region that is phosphorylated and dephosphorylated in order to deactivate and activate the protein, respectively.[32] NFAT1 activates the transcription of a number of genes during immune response. However, the three-dimensional structure of the phosphorylated region is still not well-known and might be dependent on the unusual and slow cis/trans isomerization of the numerous occurrences of XSPX motifs. We carried out several 5×10^7 steps of accelerated MD simulations on the unphosphorylated motif (TSPI) and the phosphoserine motif (TpSPI). In these studies, all-atom molecular dynamics simulations were carried out by using the Cornell et al. all-atom force field[33] and by solving the Langevin dynamics equation:

$$m\frac{d^2x}{dt^2} = F(t) - \gamma m\frac{dx}{dt} + R(t) \tag{6}$$

where γ is the collision frequency; γm is the frictional coefficient, and $R(t)$ is a random Gaussian force with zero mean. A value of 2.0 ps^{-1} was used for the collision frequency, as suggested by Loncharich et al.[34] Since conformational changes in proteins directly reflect changes in torsions, we have applied the boost to only the dihedral torsions as previously described.[14] The boost energy E was set 30.0 kcal/mol above the average total torsion energy, and the simulations were carried out at two different values of α: 15.0 and 20.0 kcal/mol. The simulations were carried out using the Sander module in the AMBER 7 suite[35] of programs that was modified to perform the accelerated molecular dynamics simulation. The modification to the Sander module involves an additional routine that calculates the forces of the atoms on the modified potential base on the conditions set in eqs 3−5. The electrostatic interaction was treated using the generalized Born implementation (igb = 2)[36] in AMBER 7, and the apolar solvation term was also included in the potential function with the surface tension parameter set to the default value of 0.005 kcal/mol Å^2. The SHAKE algorithm was applied to all bonds involving hydrogen atoms, and an integration time step of $\Delta t = 2.0$ fs was used for the integration of the Langevin equation.

Results and Discussion

Studying the cis/trans isomerization of proline using conventional molecular dynamics simulations is almost impossible because of the time scale limitations and the high energetic barrier separating the states. We have carried out several accelerated MD simulations on the unphosphorylated and phosphorylated XSPX motifs. Figure 4 shows the plot of the ω angles of the serine and proline residues of TpSPI during the course of the simulation. The top plot shows the ω angle of the *p*-serine, which stays mostly in the trans conformation. On the other hand, the bottom plot in Figure 4 shows frequent isomerization of the proline ω angle from trans to cis during the course of the simulation. The transition is shown to occur more frequently from around −180 to around 0° (anticlockwise),

(32) Hogan, P. G.; Chen, L.; Nardone, J.; Rao, A. *Genes Dev.* **2003**, *17*, 2205−2232.
(33) Cornell, W. D.; Cieplak, P.; Bayly, C. I.; Gould, I. R.; Merz, K. M.; Ferguson, D. M.; Spellmeyer, D. C.; Fox, T.; Caldwell, J. W.; Kollman, P. A. *J. Am. Chem. Soc.* **1995**, *117*, 5179−5197.
(34) Loncharich, R. J.; Brooks, B. R.; Pastor, R. W. *Biopolymers* **1992**, *32*, 523−535.
(35) Pearlman, D. A.; Case, D. A.; Caldwell, J. W.; Ross, W. S.; Cheatham, T. E.; Debolt, S.; Ferguson, D.; Seibel, G.; Kollman, P. *Comput. Phys. Commun.* **1995**, *91*, 1−41.
(36) Onufriev, A.; Case, D. A.; Bashford, D. *J. Comput. Chem.* **2002**, *23*, 1297−1304.

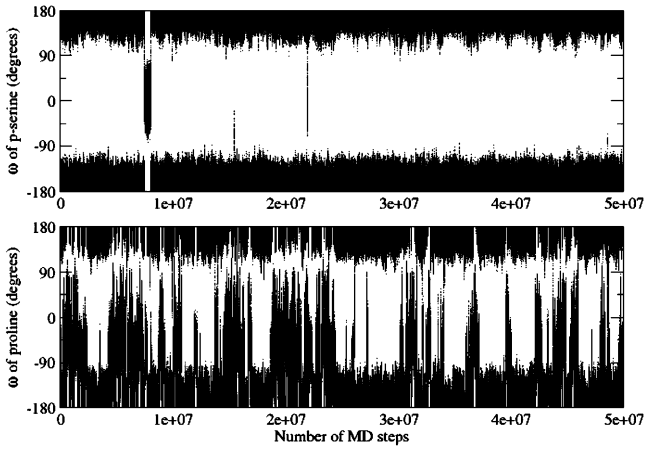

Figure 4. Variation of the ω angles of serine (top) and proline (bottom) during the course of the simulations of TpSPI.

rather than from around 180 to around 0° (clockwise). This shows that the transition from trans to cis, and vice-versa, is asymmetric and is likely characteristic of an XSPX motif. Furthermore, due to the asymmetry of the cis/trans isomerization, it could be qualitatively inferred that the barrier height for one of the transitions is lower than that of the other. Similar results were observed for the unphosphorylated TSPI motif. In agreement with our results, an earlier quantum mechanical study by Fischer et al.[31] showed that the cis/trans imide isomerization of the proline dipeptide is also asymmetric, with one energetic barrier approximately 3.0 kcal/mol higher than that of the other.

According to the study by Fischer et al.,[31] the activation barrier of the isomerization process is strongly dependent on the ψ angle of proline. Therefore, to quantitatively recapture the free energy of the barrier crossing, we have calculated the free energy surface of the barrier crossing of the cis/trans isomerization in two dimensions, as shown in Figures 5 and 6, using the ψ angle of proline as the second dimension.

The ψ backbone angle of proline in the TSPI motifs varies from around -30 (α helix) to 150° (β sheet). However, as can be seen in Figures 5 and 6, the cis/trans isomerization occurs mainly when the backbone conformation of proline is around the α-helical conformation ($\psi \sim -30$). At the cis isomer ($\omega \sim 0$), the ψ backbone angle of the proline stays mainly around the α-helical conformation and rarely gets to the β-strand region. The barrier height for the transition from the α-helical to the β-strand region, and vice versa, is much less (about 5.0 kcal/mol lower) for the trans isomer than for the cis isomer in both the phosphorylated and unphosphorylated motifs. When the backbone conformation of the proline is in the α-helical region, the barrier height for the anticlockwise trans-to-cis isomerization ($\sim$14.0 kcal/mol) of proline is similar or slightly increased after phosphorylation of the serine, in agreement with experiment, and similarly, the barrier height for cis to trans ($\sim$9.0 kcal/mol) is slightly increased with phosphorylation. As qualitatively observed in Figure 4, the second transition (clockwise) from 180 to 0° rarely occurs and has an estimated free-energy barrier of 18 kcal/mol, about 4.0 kcal/mol higher than that of the anticlockwise transition. This transition is very difficult to observe and characterize experimentally because it is much slower than the anticlockwise transition; therefore, there is no reported experimental free-energy barrier for this transition. Fischer et al.[31] estimated the activation energy (not free energy)

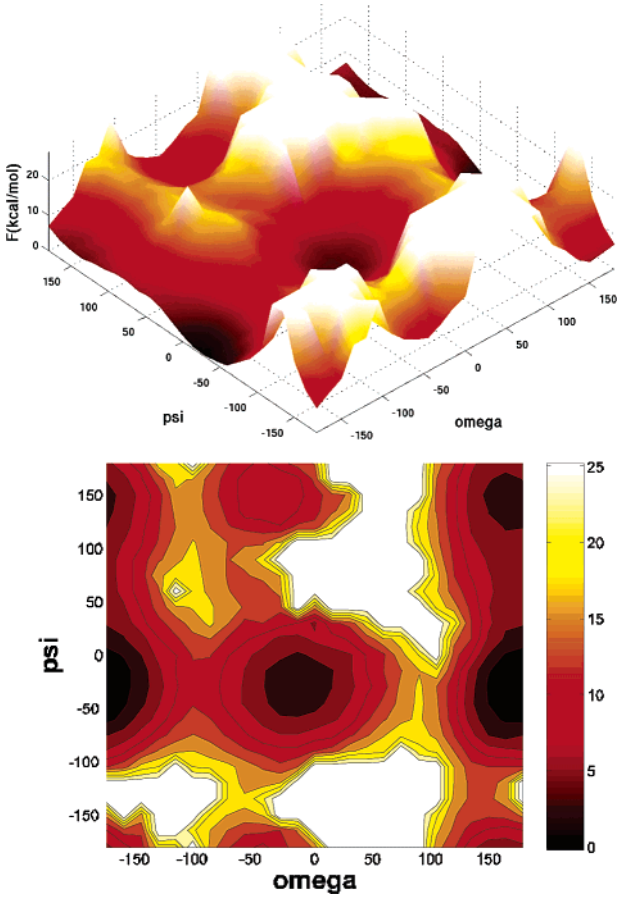

Figure 5. Free energy density plot of the cis/trans isomerization transitions along the ω and φ angles of the proline residue of the unphosphorylated TSPI motif: (top) surface plot and (bottom) contour density plot in units of kilocalories/mole.

for the higher transition of a proline dipeptide in gas phase to be around 20.7 kcal/mol.

The barrier height for the transition from the α-helical to β-strand region of the cis conformation is slightly lower for the unphosphorylated TSPI than that for the phosphorylated TpSPI motif, by about 2.5 kcal/mol. Also, when the backbone conformation of the proline is in the β-strand region, the unphosphorylated TSPI motif has a barrier height for the cis-to-trans isomerization lower than that of the phosphorylated TpSPI motif. Hence, the unphosphorylated motif can isomerize more easily from the β-strand region than can the phosphorylated motif. Therefore, it can be seen that the isomerization is strongly dependent on the ψ angle of proline and the phosphorylation state of the serine residue. The backbone angle of the proline residue is predominately in the α-helical conformation for the cis isomer.

Using the generalization of Kramers' rate theory[37] to multidimensional free-energy surfaces, put forward by Langer,[38] we have calculated the relative rate of escape for the phosphorylated and unphosphorylated TSPI motifs from trans to cis, and vice versa, for the most probable transition path, that is, when the ψ backbone angle is in the α-helical conformation (Figures 5 and

(37) Hanggi, P.; Talkner, P.; Borkovec, M. *Rev. Mod. Phys.* **1990**, *62*, 251−341.
(38) Langer, J. S. *Phys. Rev. Lett.* **1968**, *21*, 973.

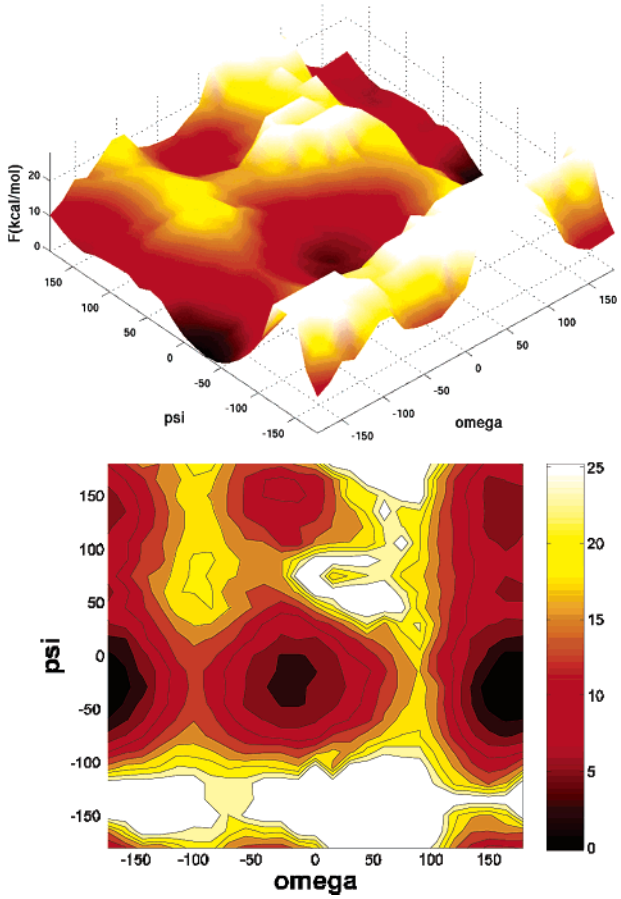

Figure 6. Free energy density plot of the cis/trans isomerization transitions along the ω and φ angles of the proline residue of the phosphorylated TpSPI motif: (top) surface plot and (bottom) contour density plot in units of kilocalories/mole.

6). The rate of escape (k) for a two-dimensional case (in this case, the ω and ψ phase space) is given by

$$k = \frac{\omega_b}{C}\frac{\omega_1^A \omega_2^A}{\omega_2^S}\exp(-F_b/k_B T) \qquad (7)$$

where ω_b and ω_2^S are the angular frequencies of the unstable and stable modes, respectively, at the transition (saddle) point; ω_1^A and ω_2^A are the angular frequencies of the modes in the metastable state A (for example, the trans or cis isomer well); F_b is the barrier height, and C is a constant. ω_b and ω_2^S were calculated by evaluating and diagonalizing the Hessian matrix at the saddle point. The ω_b and ω_2^S values are equivalent to the square roots of the eigenvalues. The ω_1^A and ω_2^A values were similarly calculated for the trans and cis wells (Figures 5 and 6). The ratio of the rate of escape ($k_{t\to c}^{unphos}/k_{t\to c}^{phos}$) of the trans isomer to cis isomer for the unphosphorylated TSPI motif relative to that of the phosphorylated TpSPI motif is estimated to be around 6. The ratio of the rate of escape ($k_{c\to t}^{unphos}/k_{c\to t}^{phos}$) for the reverse, cis to trans, is approximately 2. Therefore, both of the escape rates from the trans and cis wells decrease after phosphorylation of the serine residue. Earlier experimental studies by Schutkowski et al.[25] also showed similar results. In that study, the cis-to-trans isomerization rates of the unphosphorylated serine−proline and threonine−proline bonds ($k_{c\to t}^{unphos}$) were found to be about 2- and 8-fold faster, respectively, than

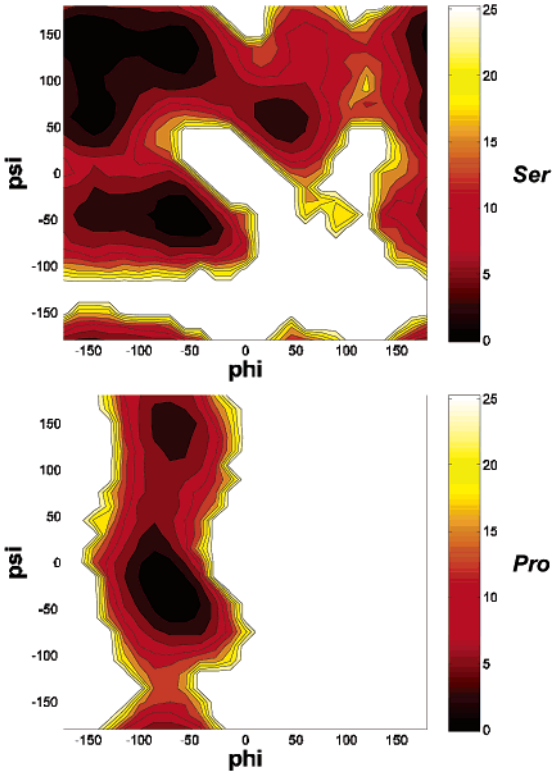

Figure 7. Reweighted density plot (in kilocalories/mole) of the ψ and φ angles of serine (top) and proline (bottom) in the unphosphorylated TSPI motif.

that of the phosphorylated analogues ($k_{c\to t}^{phos}$). According to the transition state theory and derivations by Voter,[15,16] the motions on the modified surface occur with a nonlinear effective time scale of $\Delta t_i^* = \Delta t e^{\beta \Delta V[r(t_i)]}$, where Δt is the actual time step of the simulation on the unmodified potential. However, the derivation of this equation requires that the boost potential is always zero near the saddle points; that is, the modified surface should always meet the unmodified surface near the saddle points. We do not strictly enforce this condition because the energy landscape of a biomolecule is rough, and it would require the calculation of the Hessian matrix at each step in order to detect the saddle points. Nonetheless, using a novel procedure (details to be discussed elsewhere) that relates the kinetic rates to the features of the energy landscape, we were able to estimate the rate of escape ($k_{t\to c}^{unphos}$) from the trans well to cis well for TSPI to be around 610 s^{-1} at 300 K. This calculated rate is about 2−3 orders of magnitude faster than the rates of the experiments. These fast kinetics could be attributed to the use of a much smaller collision frequency of 2.0 ps^{-1}, compared to about 60 ps^{-1} for water and the GB implicit solvation model.

Furthermore, it can be seen from the results in Figures 5 and 6 that the ψ angle of proline favors the α-helical conformation after phosphorylation. Consequently, we have also explored the dependence of the backbone conformation of the serine and proline residues of the TSPI motif before and after phosphorylation. The plot of the backbone angle of the serine and proline residues of the unphosphorylated TSPI motif is shown in Figure 7.

The backbone conformation of the serine residue is heavily populated around the α-helical ($\varphi \sim -60$, $\psi \sim -60$), the β-strand, and the polyproline II (PPII; $\varphi \sim -75$, $\psi \sim +145$) regions. The left-handed helical conformation ($\varphi \sim +60$, $\psi \sim$

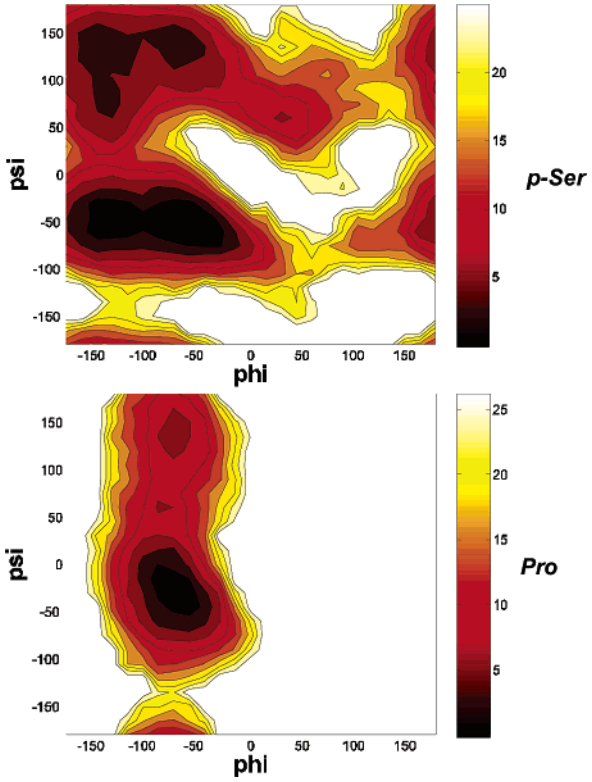

Figure 8. Reweighted density plot (in kilocalories/mole) of the ψ and φ angles of *p*-serine (top) and proline (bottom) in the phosphorylated TpSPI motif.

+50) is also sampled, but to a lesser extent. The $\varphi-\psi$ space of the proline residue is more restrictive and samples only the α-helical conformation, where $\varphi \sim -60$ and $\psi \sim -60$, and the PPII region. The α-helical conformation of the proline residue has a free energy lower than that of the PPII conformation. After phosphorylation, as shown in Figure 8, the backbone angles of the TpSPI motif tend to favor the helical conformation, similar to previously observed results with different nonproline tetrapeptide sequences.[23]

The α-helical region, where $\varphi \sim -135$ and $\psi \sim -60$, of the *p*-serine residue also becomes heavily populated, in contrast to what is seen for the unphosphorylated serine of TSPI. The two α-helical regions (double wells; Figure 8) of the *p*-serine of the phosphorylated motif have lower energies and are clearly more favored than the β-strand and PPII conformations. There is a marked decrease in the β strand, PPII, and the left-handed backbone conformations of the serine residue after phosphorylation, as is evident from Figures 7 and 8. Similarly, the α-helical region of the proline residue is more favored after phosphorylation of the serine residue.

Conclusions

With the altered energy landscape, we are able to accelerate all-atom MD substantially and recover equilibrium properties. This method allows the system to move very easily over high energy barriers in fewer computational steps than normal MD and samples energy wells that would not have been explored using normal MD. Furthermore, this method is not limited to an implicit solvation model. Preliminary ongoing calculations show that accelerated sampling is also found when using explicit water molecules. The cis/trans isomerization of the serine−proline motif is a very important conformational switching mechanism that has been implicated in many regulatory pathways. We showed that the isomerization of the ω bond of proline is asymmetric and strongly depends on the ψ-backbone conformation of proline. We have also shown that phosphorylation slows down the rate of isomerization (the unphosphorylated peptide is more fluxional) and changes the distribution of the preferred backbone conformations. While we have only examined the intrinsic isomerization and backbone behaviors and their modulation by phosphorylation, the effects that we have found are likely to contribute to the activity of enzymes, such as Pin1.

Acknowledgment. This work was supported, in part, by grants from NSF, NIH, the Center for Theoretical Biological Physics, the National Biomedical Computation Resource, San Diego Supercomputing Center, and Accelrys, Inc. We also thank John Mongan and Chenghang Zong for helpful discussions.

JA0446707